Analytical Methods

Accepted Manuscript

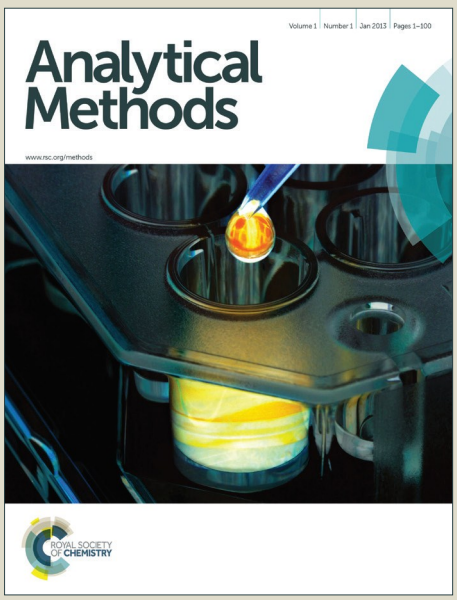

This is an *Accepted Manuscript*, which has been through the Royal Society of Chemistry peer review process and has been accepted for publication.

Accepted Manuscripts are published online shortly after acceptance, before technical editing, formatting and proof reading. Using this free service, authors can make their results available to the community, in citable form, before we publish the edited article. We will replace this *Accepted Manuscript* with the edited and formatted *Advance Article* as soon as it is available.

You can find more information about *Accepted Manuscripts* in the Information for Authors.

Please note that technical editing may introduce minor changes to the text and/or graphics, which may alter content. The journal's standard Terms & Conditions and the Ethical guidelines still apply. In no event shall the Royal Society of Chemistry be held responsible for any errors or omissions in this *Accepted Manuscript* or any consequences arising from the use of any information it contains.

ROYAL SOCIETY OF CHEMISTRY

www.rsc.org/methods

Highly sensitive and selective colorimetric detection of Hg^{2+} based on separation of Hg^{2+} and formation of catalytic DNA-gold nanoparticles

Chi-Fang Peng*, Na Pan, Zheng-Jun Xie and Liang-Liang Wu

State Key Lab of Food Science and Technology, School of Food Science and Technology, Jiangnan University

Abstract: Hg^{2+} ions can be absorbed onto DNA-AuNPs complex and separated from water samples while the catalytic activity of DNA-AuNPs can be promoted. Based on the above principle, a highly sensitive and selective colorimetric assay for the detection of Hg^{2+} was developed. The proposed method for Hg^{2+} has a detection limit of 1.5 nM with a linear range from 5.0 nM to 500 nM. Moreover, this detection method for Hg^{2+} demonstrated more than 1000-fold selectivity toward most of the possible interfering ions and can be used for tap water detection. The results indicate the high potential of AuNPs as enzyme mimic for sensing heavy metal ions by metallophilic interactions.

Introduction

Mercuric ions (Hg^{2+}) are widely distributed in the environment and have deleterious effects on the environment and human health. Monitoring Hg^{2+} level in water is a very important task in terms of water safety and water quality. The U.S. Environmental Protection Agency (EPA) has set the maximum allowable level of Hg in drinking water at 10 nM (2.0 ppb).[1] At present, there are various classical methods for detecting Hg^{2+}, including atomic fluorescence spectrometry,[2] atomic absorption

spectrometry,[3] inductively coupled plasma mass spectrometry,[4] These methods are selective and sensitive, but require expensive instruments and complicated sample pretreatments.[5]

In order to overcome these problems, many metallic nanoparticle-based sensors have been developed.[6-15] In these nanosensors, various specific ligands of Hg^{2+} were carefully selected to achieve selective respond to Hg^{2+}. For example, DNA-gold nanoparticle (AuNP) assays have demonstrated excellent selectivity for Hg^{2+} that can interact with T-T mismatches to form T-Hg^{2+}-T complexes.[8-10, 15] Many small ligands, including (11-mercapto-undecyl)-trimethyl-ammonium, mercaptopropionic acid,[13] homocystine, lysine,[14] diethyldithiocarbamate,[6] 5-methyl-2-thiouracil,[12] dithiocarbamate derivative of calixarene,[7] and 1-dodecanethiol,[11] modified on the surface of AuNPs also have demonstrated specific interaction with Hg^{2+}. This ligand-mediated interaction can be measured by fluorescent, colorimetric, chemiluminescent, electrochemical and electrochemiluminescent methods, etc.[6, 11, 14, 16-18] Interestingly, Hg^{2+} also can interact strongly and selectively with gold nanoparticles,[19] gold nanorods[5] and silver nanoparticles,[20] which results in forming Au/Hg and Ag/Hg alloys (amalgam). This specific metallophilic interaction[21] has been used to develop fluorescent and colorimetric sensors of Hg^{2+}.[5, 19, 20, 22, 23] Although most of these methods have demonstrated high sensitivity to Hg^{2+} and good selectivity to other common metal ions, it is still difficult to eliminate the interference from the high concentration of various metal ions in real samples without proper sample purification. In order to solve this problem, some specific materials, such as YPA4 resin microcolumn and Hg^{2+}-imprinted polymers,[24, 25] were prepared to separate or preconcentrate Hg^{2+} from real samples.

Recently, some methods for Hg^{2+} detection were developed based on the formation of Hg-Au alloy NPs which possess higher peroxidase-like activity than naked AuNPs. For example, Long *et al.*[23] utilized the above Hg-Au alloy NPs to catalyze TMB-H_2O_2 redox reaction and developed a colorimetric assay for Hg^{2+} detection. Yan *et al.*[22] and Wang *et al.*[26] developed fluorescent detections of Hg^{2+} on the basis of the oxidation of o-phenylenediamine and Amplex UltraRed, catalyzed by the above Au-Hg peroxidase-mimic. Although these methods have demonstrated excellent analytical performance for Hg^{2+} detection, the high concentration of other metal ions in samples may produce serious matrix interference. Improving the selectivity and sensitivity of Hg^{2+}detection is an effective strategy to avoid matrix effects.

In this work, we improved Long's method for Hg^{2+} detection by using a DNA-AuNPs complex. In our strategy, Hg^{2+} ions were deposited onto DNA-AuNPs complex and separated from water samples, and then quantified by measuring the catalytic activity of the formed Au/Hg amalgam. This new method has several advantages: (i) The selectivity of this detection for Hg^{2+} was outstanding due to the combination of the metallophilic interaction of Au-Hg and further separation of Au-Hg amalgam through centrifugation. (ii) This proposed method was highly sensitive with a detection limit of 1.5 nM and a linear range from 5.0 nM to 500 nM. The sensitivity of this method is satisfactory for environmental water samples. (iii) The preparation of DNA- AuNPs complex is simple and the detection is low-cost.

Experimental Section

Reagents and chemicals

Hydrogen tetrachloroaurate (III) tetrahydrate ($HAuCl_4 \cdot 4H_2O$) were purchased from Aldrich (Milwaukee, WI). Trisodium citrate ($Na_3C_6H_5O_7 \cdot 2H_2O$) and citric acid monohydrate ($C_6H_8O_7 \cdot H_2O$) were obtained from Sigma (St. Louis, MO). The thiolated single strand oligonucleotides, 5'-SH-TTTTTTTTTT-3' (T_{10}) and 5'-SH-GCGACATGGTAATGG-3' (a random sequence, rDNA), were purchased from Sangon Biotech (Shanghai) Co., Ltd. $Hg(NO_3)_2$ and all the other metal salts were purchased from the national institute of metrology P. R. China standard. 3, 3, 5, 5-tetramethylbenzidine (TMB) was supplied by Sinopharm Group Chemical Regent Co., Ltd (Shanghai, China). All of the reagents used were of analytical grade. Ultra-pure water prepared with a Milli-Q Pure system was used throughout the experiments.

Synthesis of AuNPs

AuNPs were prepared through citrate-mediated reduction of $HAuCl_4$.[27] Firstly, 0.01% chloroauric acid solution (100 mL) was added to a flask which had been soaked with aqua regia solution and cleaned with ultra-pure water. Then the flask was stirred and heated until boiling for 10 min. 1.0% sodium citrate (2.0 mL) was subsequently added quickly to the boiling solution. An obvious color change of the reaction mixture was observed from transparent to dark blue and finally wine red. The mixture was further boiled for another 5 min and cooled to room temperature.

Preparation of DNA-AuNP complex

The DNA-functionalized Au nanoparticles were prepared by directly incubating the thiolated DNA strands with AuNP solution. Firstly, the prepared AuNP solution (3 nM) was concentrated to 6 nM by centrifugation. Then the concentrated AuNPs (6 nM, 990 μL) were mixed with thiolated DNA (100 μM, 10 μL). After incubated at 25°C for 24 h, the mixtures were centrifuged for 15 min at 10000 rpm and the excess

DNA was removed. After repeating the centrifugation for twice the obtained DNA-AuNP complex was resuspended in ultra-pure water and stored at 4°C.

Analytical procedure for the colorimetric detection of Hg^{2+}

Different concentrations of Hg^{2+} (500 μL) were mixed with DNA-AuNPs solution (0.6 nM, 25 μL) and trisodium citrate (8 mM, 175 μL), and then incubated for 30 min at room temperature. Then the mixtures were centrifuged at 10000 rpm for 15 min and the supernatants were removed, by which 50 μL of concentrated solution was obtained. Afterward, 90 μL of citrate buffer (100 mM, pH 4.5), 100 μL of TMB (1.5 mM) and 60 μL of H_2O_2 (1.5 M) were pipetted into the above concentrated solution. The absorbance value of the mixture was then measured at 650 nm by a microplate reader (PowerWave XS2, Bio-Teck, USA).

Results and discussion

Characterization of AuNPs and DNA-AuNPs complex

The dimension of the AuNPs was measured with a transmission electron microscope (TEM, H7100, Hitachi High-Technologies Corporation, Tokyo, Japan). The AuNPs were monodisperse with an average size of 16 nm (Figure S1). The concentration of AuNPs was estimated to be 3.0 nM. Hg^{2+} can be absorbed by AuNPs through strong Au-Hg metallophilic interaction, but the formed Au/Hg alloy is unstable.[19] In order to separate Hg^{2+} from solution, AuNPs should be protected and stabilized by some molecules.[19] Considering that AuNPs can be modified controllably with thiolated DNA, a DNA-AuNP complex was prepared and used to separate Hg^{2+} ions.

Figure 1 shows the UV-vis absorption spectra of the AuNPs with a maximum absorption peak (λmax) at 519 nm. After AuNPs modified with T_{10}, the λmax

red-shifted from 519 nm to 522 nm. These results confirmed the successful conjugation of AuNPs and DNA strands. After T_{10}-AuNPs were incubated with a high concentration of Hg^{2+}(500 nM), the λmax blue-shifted from 522 nm to 520 nm, which should attribute to that Hg^{2+} ions were reduced to Hg^0 and then adsorbed onto the surface of the DNA-AuNPs.[28] It should be noted that the spectrum of DNA-AuNPs kept almost unchanged in terms of intensity and shape after incubated with high concentration of Hg^{2+}. The TEM images of AuNPs , T_{10}-AuNPs and T_{10}-AuNPs treated with Hg^{2+} (500 nM) also showed that all three kinds of Au NPs are mono-dispersed (Figure S1).

The above result confirmed the high stability of DNA-AuNPs/Hg^{2+} complex that will be beneficial to the separation of Hg^{2+} from water samples.

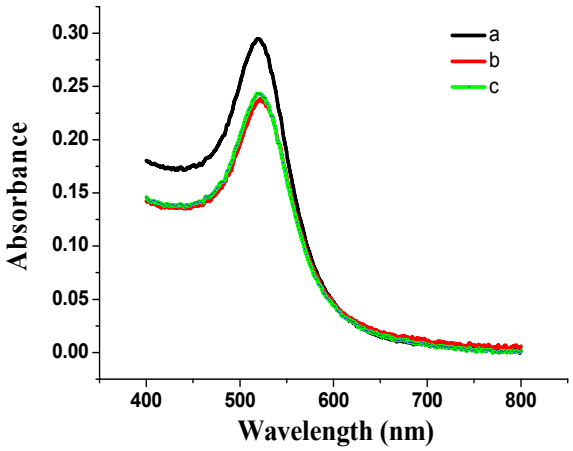

Figure 1. UV-Vis spectra of (a) AuNPs, (b) T_{10}-AuNPs and (c) T_{10}-AuNPs treated with Hg^{2+} (500 nM).

Effects of DNA on the detection of Hg^{2+}

Long *et al.*[23] found that the forming of Hg-Au alloy NPs stimulated the catalytic ability of Au NPs to TMB-H_2O_2 redox reaction by accelerating the decomposition of

H_2O_2. Here this mechanism can be used to detect Hg^{2+} further after Hg^{2+} was separated from water sample by DNA-AuNPs.

To confirm that the redox reaction between TMB and H_2O_2 was accelerated by the formed Hg–Au alloys, the UV-Vis spectra were recorded separately in the presence of AuNPs, T_{10}-AuNPs, AuNPs/Hg^{2+} and T_{10}-AuNPs/Hg^{2+}. As shown in Figure 2, the absorbance value at 650 nm (A_{650}) in the presence of AuNPs or T_{10}-AuNPs is very low, indicating their very weak catalysis toward the redox reaction of TMB-H_2O_2 (curve a and curve b in Figure 2). However, this redox reaction can be catalyzed by AuNPs/Hg^{2+} system obviously (curve c in Figure 2), indicating the catalytic capacity promotion of AuNPs by Hg^{2+}. Moreover, the catalytic capacity of the T_{10}-AuNPs can be promoted almost the same as that of the AuNPs (curve d in Figure 2).

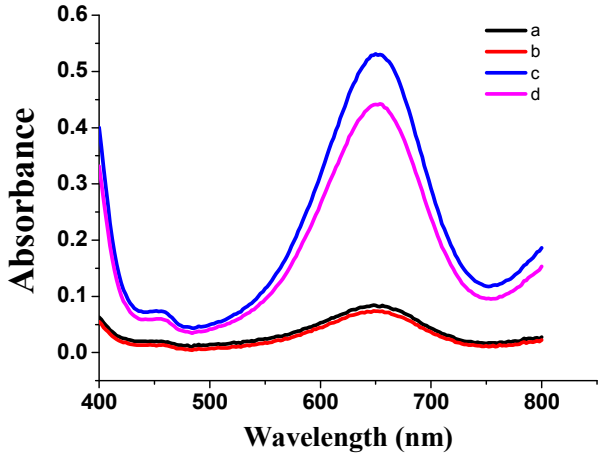

Figure 2. UV−vis spectra of TMB and H_2O_2 after incubation with different catalytic system: (a) AuNPs; (b) T_{10}-AuNPs; (c) AuNPs + Hg^{2+} (500 nM); (d) T_{10}-AuNPs + Hg^{2+} (500 nM).

The AuNPs modified with T_{10} (T_{10}-AuNPs) or a random ssDNA (rDNA-AuNPs) were utilized to separate and detect Hg^{2+} ions. As expected, the absorbance values at 650 nm (A_{650}) increased rapidly as the increasing of Hg^{2+} concentrations in the range

of 50-500 nM when the T_{10}-AuNPs complex was utilized to separate and detect Hg^{2+} (Figure 3). In contrast, the A_{650} increased slowly when AuNPs without modification of DNA were used. In the case of the rDNA-AuNPs complex, the A_{650} increased more rapidly over the range 10-250 nM than that of T_{10}-AuNPs. However, the A_{650} started to decline as the Hg^{2+} concentration increased above 250 nM.

It was known that T_{10} and Hg^{2+} can interact and form T-Hg^{2+}-T complex, which probably reduced the absorption of Hg^{2+} on the surface of AuNPs. Meanwhile, it was reported that T_n sequences possess more extended and upright conformations on the surface of AuNPs than rDNA.[29] The different performance between rDNA-AuNPs and T_{10}-AuNPs in the sensing of Hg^{2+} should be due to the different interaction of DNA srands and Hg^{2+} as well as the different conformations of T_{10} and rDNA sequences on the surface of AuNPs. Considering the sensitivity and a wide linear respond to Hg^{2+} concentration, T_{10}-AuNPs complex was selected for the next experiment.

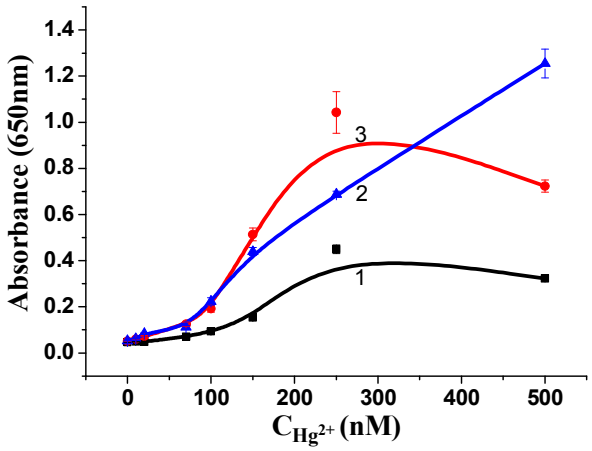

Figure 3. Effect of DNA on the colorimetric detection for Hg^{2+}. The TMB-H_2O_2 redox reaction catalyzed by citrate-capped AuNPs (1), T_{10}-AuNPs (2) and rDNA-AuNPs (3) after the addition of various concentrations of Hg^{2+} ions (0, 10, 20, 70, 100, 150, 250 and 500 nM). The concentration

of AuNPs, T_{10}-AuNPs and rDNA-AuNPs, 0.6 nM; TMB, 1 mM; H_2O_2, 1.5 M; pH, 4.5; reaction time, 25 min.

Since macromolecules on the metallic nanoparticles can affect their catalytic activity,[30] the concentrations of T_{10} used to modify the AuNPs were investigated. It was found that the T_{10}-AuNPs showed highest catalytic activity when 1.0 μM of T_{10} was utilized (Figure S2).

Effect of Hg^{2+} volume

Overall, the catalytic activity of T_{10}-AuNPs increased with increasing the Hg^{2+} volume from 100 μL to 1000 μL. As a result, sharper respond to Hg^{2+} concentration occurred when bigger volume of Hg^{2+} solution was utilized to detect Hg^{2+} (Figure 4). However, a shoulder peak appeared when using 1000 μL of Hg^{2+} solution for Hg^{2+} detection. This phenomenon should be due to the excessive deposition of Hg^{2+} onto the surface of the T_{10}-AuNPs complex, which led to destabilization of the T_{10}-AuNPs complex. A wide linear range of 10-500 nM can be obtained whether 100 μL or 500 μL of Hg^{2+} was mixed with the T_{10}-AuNPs complex, but much higher sensitive respond was found with 500 μL of Hg^{2+} used than 100 μL of Hg^{2+}.

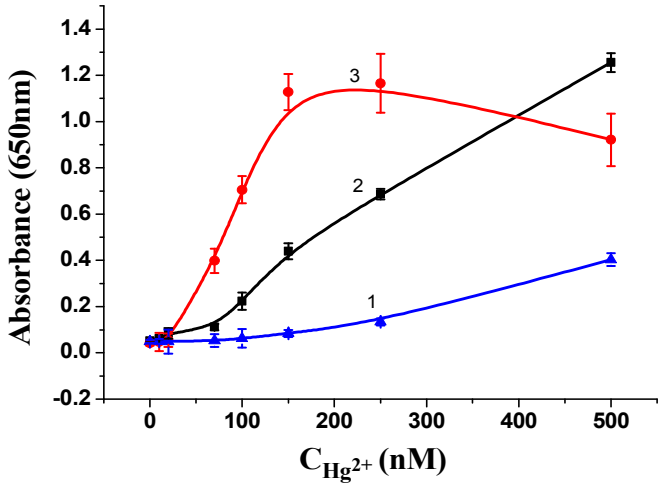

Figure 4. The colorimetric detection for Hg^{2+} by T_{10}-AuNPs after incubated with different volume of Hg^{2+} (From 1 to 3, the volumes of Hg^{2+} were: 100 μL, 500 μL and 1000 μL, respectively. The concentrations of Hg^{2+} were 0, 10, 20, 70, 100, 150, 250 and 500 nM, respectivey). T_{10}-AuNPs, 0.6 nM; TMB, 1.0 mM; H_2O_2, 1.5 M; pH, 4.5; reaction time, 25 min.

Sensitivity and selectivity of the detection of Hg^{2+}

Several parameters including the concentrations of TMB and H_2O_2 and reaction time were investigated to optimize the conditions for the colorimetric detection of Hg^{2+} ions. As shown in Figure S3, the A_{650} increased as reaction time increasing and reached a plateau after 20 min. In Figure S4, it can be seen that the highest A_{650} was found at 1.5 M over the range of 0.9-1.5 M H_2O_2. The maximal difference of absorbance values in the presence and absence of Hg^{2+} was achieved at 1.5 M of H_2O_2.

In the presence of 200 nM Hg^{2+}, the A_{650} increased sharply with increasing the concentration of TMB in the range of 0.1-1.0 mM and then reached a plateau at 1.5 mM TMB (Figure S5). The highest A_{650} was found at 0.6 nM of T_{10}-AuNPs over the range 0.2-3.0 nM (Figure S6). In addition, the background signal increased with the increasing concentration of T_{10}-AuNPs.

Under the optimal conditions, Hg^{2+} level as low as 20 nM can be clearly detected by the naked eye and a calibration curve for Hg^{2+} detection was obtained with a linear range from 5 nM to 500 nM (R^2 = 0.993) (Figure 5). The limit of detection was estimated to be 1.5 nM at a signal-to-noise ratio of 3, which was more sensitive than most of previously reported colorimetric and some of the fluorescent methods (some representative methods were listed in Table S1).[5-9, 13, 14, 17, 22, 26, 31, 33, 34]

To investigate the selectivity of the T_{10}-AuNPs probe (0.6 nM) toward Hg^{2+}, 10 μM Mg^{2+}, Ca^{2+}, Sr^{2+}, Ni^{2+}, Cu^{2+}, Zn^{2+}, Mn^{2+}, Cr^{3+}, Cd^{2+}, Al^{3+}, Co^{2+}, Bi^{3+}, Ba^{2+}, Pb^{2+} or

Fe^{3+} was added into the T_{10}-AuNPs, separately. As a control, we added 20.0 nM and 200 nM Hg^{2+} ions into the probe solutions. Figure 6 reveals that only mercury can stimulate the peroxidase-like activity of the AuNPs. As expected, the tolerance of the T_{10}-AuNPs probe for Hg^{2+} ions toward most of the possible interfering ions was more than 1000-fold except that it was more than 500-fold toward Ca^{2+}. The selectivity of our method for Hg^{2+} detection was higher than most of the reported colorimetric methods.[5, 7, 19, 23, 31, 32] This high selectivity should be due to the selective separation of Hg^{2+} from water as well as the consequent Hg^{2+}-stimulated the peroxidase-like activity of AuNPs.

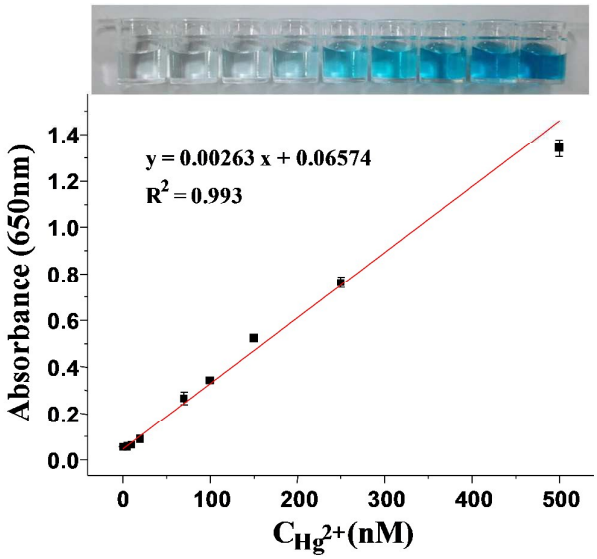

Figure 5. Photographic images of the colors and calibration curve for the detection of Hg^{2+} after the addition of various concentrations of Hg^{2+} ions (0, 5, 10, 20, 70, 100, 150, 250 and 500 nM). T_{10}-AuNPs, 0.6 nM; TMB, 1.5 mM; H_2O_2, 1.5 M; pH, 4.5; reaction time, 20 min.

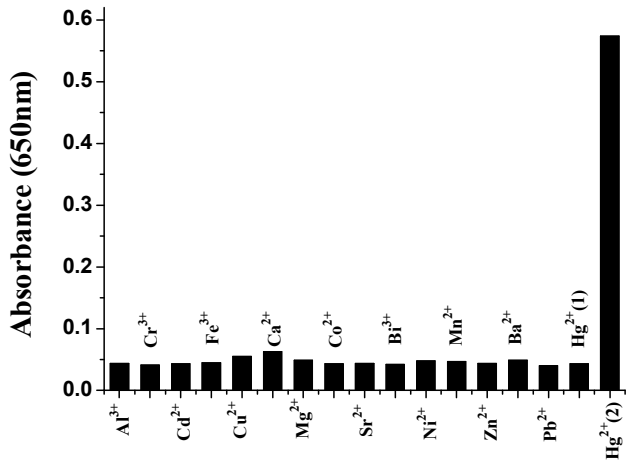

Figure 6. Catalytic activity of T_{10}-AuNPs stimulated by various metal ions. All metal ions are 10 μM except for Hg^{2+} (1) (20 nM) and Hg^{2+} (2) (200 nM). T_{10}-AuNPs, 0.6 nM; TMB, 1.5 mM; H_2O_2, 1.5 M; pH, 4.5; reaction time, 20 min.

Detection of Hg^{2+} ions in tap water samples

To test the practicality of the proposed method, the T_{10}-AuNPs were used to detect Hg^{2+} ions in tap water. The tap water samples collected from our laboratory were detected by atomic fluorescence spectrometry and the concentration of Hg^{2+} was lower than 2.5 nM. After aliquots of tap water were spiked with 10, 50 and 200 nM Hg^{2+} ions, respectively, the samples were filtered through microfiltration membranes and measured by our method. The recoveries of 90.9-112.0% with relative standard deviation (RSD) of 2.0-8.9% were shown in Table 1. The results demonstrated that the proposed colorimetric method can accurately and reliably determine Hg^{2+} in real samples.

Table 1. Determination of Hg^{2+} in tap water samples (n = 3)

Added Hg^{2+} (nM)	Found Hg^{2+} (nM)	Recovery (%)	RSD (%)
10	11.2	112.0	8.9
50	53.1	106.2	2.0

200	181.8	90.9	7.6

Conclusions

A highly sensitive and selective colorimetric assay for the detection of Hg^{2+} ions was developed based on the simple separation of Hg^{2+} by DNA-AuNPs and the Hg^{2+}-stimulated the peroxidase-like activity of AuNPs. The DNA strands modified on the surface of AuNPs can stabilize the Au-Hg alloy NPs and keep their peroxidase-like activity. The proposed method has a detection limit of 1.5 nM Hg^{2+} with a linear range from 5.0 nM to 500 nM. Moreover, the above method of Hg^{2+} detection showed ultra-high selectivity toward other common metal ions. The developed colorimetric method opens up a new possibility for monitoring trace level of heavy metal ions in water samples.

Acknowledgements

The work was supported by the National S&T support program of China (2015BAD17B02), the National Natural Science Foundation of China (31371767), and the Natural Science Foundation of Jiangsu Province (BK20141108).

Notes and references

1 EPA 816-F-09-0004, U.S. EPA, 2009

2 Z. Zhu, L. Xu, X. Zhou, J. Qin and C. L. Yang, *Chem. Commun.*, 2011, **47**, 8010-8012.

3 C. K. Chiang, C. C. Huang, C.-W. Liu and H. T. Chang, *Anal. Chem.*, 2008, **80**, 3716-3721.

4 D. M. Kong, N. Wang, X. X. Guo and H. X. Shen, *Analyst*, 2010, **135**, 545-549.

5 L. H. Jin and C. S. Han, *Sensors and Actuators B: Chemical*, 2014, **195**, 239-245.

6 L. Chen, J. Li and L. X. Chen, *ACS Appl. Mater. Interfaces*, 2014, **6**, 15897-15904.

7 M. Debdeep, K. Anshu, G. Ravi and P. Parimal, *Colloids and Surfaces A Physicochem. Eng. Aspects*, 2014, **455**, 122-128.

8 C. W. Liu, C. C. Huang and H. T. Chang, *Langmuir*, 2008, **24**, 8346-8350.

9 C. W. Liu, Y. T. Hsieh, C. C. Huang, Z. H. Lin and H. T. Chang, *Chem. Commun.*, 2008, **18**, 2242-2244.

10 J. H. Huang, X. Gao, J. J. Jia, J. K. Kim and Z. G. Li, *Anal. Chem.*, 2014, **86**, 3209-3215.

11 L. Chen, X. L. Fu, W. H. Lu and L. X. Chen, *ACS Appl. Mater. Interfaces*, 2013, **5**, 284-290.

12 N. Zhou, H. Chen, J. H. Li and L. X. Chen, *Microchim Acta*, 2013, **180**, 493-499.

13 D. B. Liu, W. S. Qu, W. W. Chen, W. Zhang, Z. Wang and X. Y. Jiang, *Anal. Chem.*, 2010, **82**, 9606-9610.

14 S. Gulsu, U. Lokman and D. Adil, *Anal. Chem.*, 2014, **86**, 514-520.

15 L. Chen, T. T. Lou, C. W. Yu, Q. Kang and L. X. Chen, *Analyst*, 2011, **136**, 4770-4773.

16 J. H. Chen, S. G. Zhou and J. L. Wen, *Anal. Chem.*, 2014, **86**, 3108-3114.

17 C. C. Huang and H. T. Chang, *Anal. Chem.*, 2006, **78**, 8332-8338.

18 S. Cai, K. Lao, C. W. Lau and J. Z. Lu, *Anal. Chem.*, 2011, **83**, 9702-9708.

19 C. Y. Lin, C. J. Yu, Y. H. Lin and W. L. Tseng, *Anal. Chem.*, 2010, **82**, 6830-6837.

20 L. Deng, X. Y. Ouyang, J. Y. Jin, C. Ma, Y. Jiang, J. Zheng, J. S. Li, Y. H. Li, W. H. Tan and R. H. Yang, *Anal. Chem.*, 2013, **85**, 8594-8600.

21 M. Fernando, M. Sebastian and B. Lorena, *Physical Chemistry Chemical Physics*, 2015, **17**, 26417-26428.

22 L. Yan, Z. P. Chen, Z. Y. Zhang, C. L. Qu, L. X. Chen and D. Z. Shen, *Analyst*, 2013, **138**, 4280-4283.

23 Y. J. Long, Y. F. Li, Y. Liu, J. J. Zheng, J. Tang and C. Z. Huang, *Chem. Commun.*, 2011, **47**, 11939-11941.

24 S. F. Xu, L. X. Chen, J. H. Li, Y. F. Guan and H. Z. Lu, *J. Hazard. Mater.*, 2012, **237–238**, 347-354.

25 C. M. Xiong and B. Hu, *J. Agric. Food Chem.*, 2007, **55**, 10129-10134.

26 C. I. Wang, C. C. Huang, Y. W. Lin, W. T. Chen and H. T. Chang, *Analytica chimica acta*, 2012, **745**, 124-130.

27 Z. Mei, H. Chu, W. Chen, F. Xue, J. Liu, H. Xu, R. Zhang and L. Zheng, *Biosens. Bioelectron.*, 2013, **39**, 26-30.

28 G. L. Wang, X. Y. Zhu, H. J. Jiao, Y. M. Dong and Z. J. Li, *Biosens. Bioelectron.*, 2012, **31**, 337-342.

29 W. Li, Y. F. Dong, X. Wang, H. Li and D. K. Xu, *Biosens. Bioelectron.*, 2015, **66**, 43-49.

30 C. L. Li, C. C. Huang, W. H. Chen, C. K. Chiang and H. T. Chang, *Analyst*, 2012, **137**, 5222-5228.

31 G. H. Chen, W. Y. Chen, Y. C. Yen, C. W. Wang, H. T. Chang and C. F. Chen, *Anal. Chem.*, 2014, **86**, 6843-6849.

32 G. L. Wang, L. Y. Jin, X. M. Wu, Y. M. Dong and Z. J. Li, *Analytica chimica acta*, 2015, **871**, 1-8.

33 Z. q. Tan and J. f. Liu, *Anal. Chem.*, 2010, **82**, 4222-4228.

34 G. K. Darbha, A. K. Singh, U. S. Rai, E. Yu, H. T. Yu and C. R. Paresh, *J. Am. Chem. Soc.* , 2008, **130**, 8038-8043.

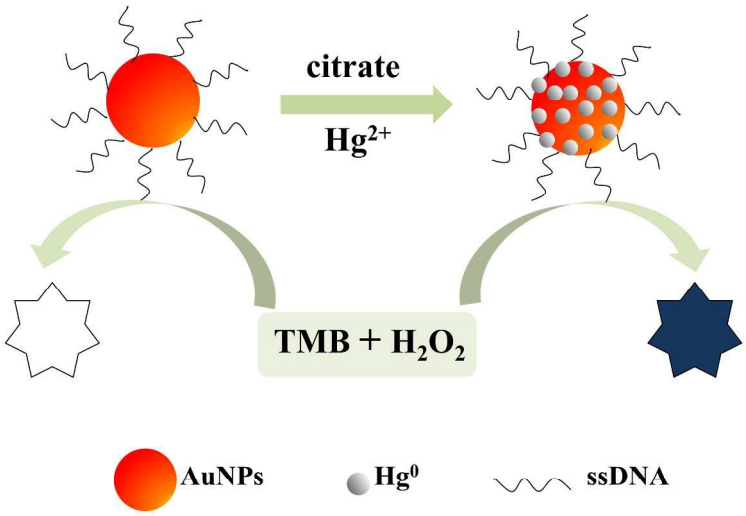

754x570mm (96 x 96 DPI)